Al⁺ Activates Acetone to Form Pinacolate

Apakorn Phasuk and Ricardo B. Metz*

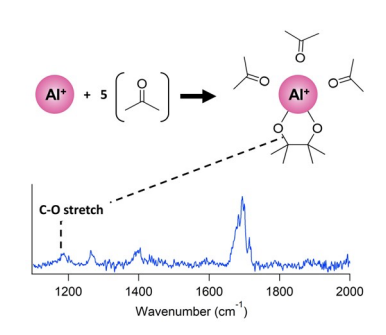
Department of Chemistry, University of Massachusetts Amherst, Amherst, Massachusetts 01003,
United States

rbmetz@chem.umass.edu

ABSTRACT

The interaction between aluminum cations and acetone is studied in the gas phase via photodissociation vibrational spectroscopy from 1100 to 2000 cm $^{-1}$. Spectra of Al⁺(acetone)(N₂) and ions with the stoichiometry of Al⁺(acetone)_n (n=2-5) were measured. The experimental results are compared to DFT calculated vibrational spectra to determine the structures of the complexes. The spectra show a red shift of the C=O stretch and a blue shift of the CCC stretch which decrease as the size of the clusters increases. The calculations predict that the most stable isomer for n \geq 3 is a pinacolate in which oxidation of the Al⁺ enables reductive C-C coupling between two acetone ligands. Experimentally, pinacolate formation is observed for n=5, as evidenced by a new peak observed at 1185 cm $^{-1}$ characteristic of the pinacolate C-O stretch.

TOC GRAPHIC



KEYWORDS Reductive C-C coupling; vibrational spectroscopy; pinacol; photodissociation; solvent distortion

The reaction to form a vicinal carbon-carbon bond between the carbonyl group of an aldehyde or ketone substrate in the presence of an electron donor is a useful synthetic method called the pinacol coupling reaction (reductive dimerization of carbonyl compound). Compounds of several lowvalent metals, such as V, Zn, Ti, Sm, Mg and Al, have been studied as catalysts for this reaction.²⁻ ⁴ Recent work has focused on main group elements, especially Mg and Al, due to their reduced toxicity and high abundance. For example, Li and Chan⁵ carried out pinacol coupling reactions in aqueous media using Al metal and fluoride salts. Acetone is the smallest ketone and has been used as a common solvent and substrate in many organic reactions including as a substrate in the pinacol coupling reaction. The interactions of acetone in bulk reactions is difficult to control, characterize, or predict on the molecular scale due to their complexity. On the other hand, gas-phase sizeselected clusters provide a versatile platform in which to study reactions, as they are amenable to highly sensitive characterization techniques and detailed calculations.⁷ In particular, coupled mass spectrometry with vibrational IR spectroscopy, in conjunction with computational quantum chemistry calculations, is an excellent tool for structural characterization of gas-phase cluster ions.⁸ There have been a few studies of ions containing acetone. Velasquez et al.9 measured spectra of M⁺(Ace)(Ar) for M=Ca, Mg and Al (Ace=acetone) from 1550 to 1850 cm⁻¹ to study the effect of the metal on the C=O stretching frequency. Meanwhile, Groenewold et al.¹⁰ investigated UO₂²⁺(ligand)_n complexes with acetone and acetonitrile in from 900 to 1850 cm⁻¹ to examine the effect of ligands on the uranyl stretching frequencies and the effect of the uranyl on the ligand vibrations. They observe that the C=O stretch in acetone red shifts, with the larger shifts for smaller clusters. He and his co-workers also observe similar results in complexes of [CeOH]²⁺ ligated by three and four acetones.¹¹ There is no evidence for pinacolate (Pin) formation in these studies. However, Duncan and co-workers observed coupling of CO₂ to make oxalate, in V⁺(CO₂)_n clusters, but do not observe oxalate formation for Al⁺(CO₂)_n.^{12,13} This is analogous to the pinacol reaction, as it couples electron transfer and C-C bond formation in carbonyl substrates. Reinhard et al.¹⁴ observed reductive C-C coupling in Nb⁺(acetonitrile)₅ but not in smaller clusters.

Here, we study the interactions between Al cation and acetones as the representative ketone to understand the system. Key questions for this work are: What is the structure of the complexes? How does the interaction with the metal affect bonds in acetone? Does the pinacol reaction take place in these clusters? If so, how many acetones are required? In this study, we investigate the structures and bonding interactions in these systems by measuring the vibrational spectra of size-selected cluster ions from 1100-2000 cm⁻¹ and carrying out DFT calculations of their structures and spectra.

A typical mass spectrum produced by laser ablation of aluminum in a mixture of acetone vapor, argon and helium is shown in figure S1. The major peaks are assigned to ions with the mass of Al⁺(Ace)_n. The distribution depends on the concentration of acetone in the gas mixture, with higher concentration favoring larger clusters; no magic numbers are observed.

Al⁺(Ace)_n. The binding energy of acetone to Al⁺ is calculated to exceed 15000 cm⁻¹ (Table 1), and no dissociation of Al⁺(Ace) is observed. Instead, the spectrum of the nitrogen-tagged complex, Al⁺(Ace)(N₂) was measured, monitoring loss of N₂. The larger clusters Al⁺(Ace)_n (n=2-5) photodissociate, and their spectra were obtained by monitoring loss of one or more acetone, the only products observed. The calculated binding energies of these complexes all exceed 3000 cm⁻¹, so all of the fragments observed are due to infrared multiple-photon dissociation (IRMPD). It is surprising that IRMPD is so efficient at the low laser fluences in this study, but IRMPD is likely

facilitated by multipassing the IR beam and by efficient intramolecular vibrational relaxation in the clusters.

Table 1. Calculated Binding Energies of $Al^+(Ace)(N_2)$ and stoichiometric $Al^+(Ace)_n$ (n = 1-5).

Species	B3LYP+D3		ωB97X-D	
	cm ⁻¹	kJ/mol	cm ⁻¹	kJ/mol
$Al^+(Ace) \rightarrow Al^+ + Ace$	15221	182.1	15416	184.4
	14512	173.6ª	15440	184.7°
	14938	178.7 ^b	14796	(expt)177.0 ^d
$Al^+(Ace)(N_2) \rightarrow Al^+(Ace) + N_2$	901	10.8	788	9.4
$Al^{+}(Pin) \rightarrow Al^{+}(Ace) + Ace$	-9059	-108.4	-7230	-86.5
$Al^+(Ace)_2 \rightarrow Al^+(Ace) + Ace$	8978	107.4	9310	111.4
	9722	116.3e	9898	(expt)118.4 ^f
$Al^{+}(Pin)(Ace) \rightarrow Al^{+}(Pin) + Ace$	28921	346.0	30266	362.1
\rightarrow Al ⁺ (Ace) ₂ + Ace	10885	130.2	13726	164.2
$Al^+(Ace)_3 \rightarrow Al^+(Ace)_2 + Ace$	6493	77.7	7221	86.4
$Al^+(Pin)(Ace)_2 \rightarrow Al^+(Pin)(Ace) + Ace$	18552	221.9	19285	230.7
\rightarrow Al ⁺ (Ace) ₃ + Ace	22943	274.5	25791	308.5
$Al^{+}(Ace)_4 \rightarrow Al^{+}(Ace)_3 + Ace$	9984	119.4	9989	119.5
$Al^{+}(Ace)_{3}(Ace) \rightarrow Al^{+}(Ace)_{3} + Ace$	3843	46.0	4010	48.0
$Al^{+}(Ace)_{2}(Ace)_{2} \rightarrow Al^{+}(Ace)_{2}(Ace) + Ace$	3304	39.5	N/A	N/A
$Al^+(Pin)(Ace)_3 \rightarrow Al^+(Pin)(Ace)_2 + Ace$	8532	102.1	9064	108.4
$Al^{+}(Pin)(Ace)_{2}(Ace) \rightarrow Al^{+}(Pin)(Ace)_{2} + Ace$	4904	58.7	4887	58.5
$A1^{+}(Pin)(Ace)_{2}(Ace)' \rightarrow A1^{+}(Pin)(Ace)_{2} + Ace'$	3914	46.8	3858	46.2
$Al^+(Ace)_5 \rightarrow Al^+(Ace)_4 + Ace$	6777	81.1	7409	88.6

Calculations performed at zero Kelvin with the 6-311+G(d,p) basis set unless indicated otherwise. For Al⁺(Pin)_m (Ace)_n(Ace)_k, the (Ace)_k indicates second-shell acetone ligands. ^a reference ¹⁵, HF/TZ2P. ^b reference 9, B3LYP/6-311+G(d,p). ^c reference ¹⁶, calculated at G4 level. ^d reference ¹⁷, experimental value, ΔH_{298} . ^e reference ¹⁵, HF/DZ. ^f reference ^{15,17}, experimental value, ΔH_{298} .

The infrared photodissociation spectra of ions with the stoichiometry of $Al^{+}(Ace)(N_{2})$ and $Al^{+}(Ace)_{2.5}$ are shown in figure 1. The spectra show a red shift in the C=O stretch which decreases as the size of the cluster increases. For n=4, there are two peaks in the C=O stretching region, and for n=5, there are multiple, partially-resolved peaks. The Al^{+} binds to the carbonyl oxygen. This weakens the C=O bond, leading to a substantial red shift in its stretching frequency and enhancing its already large IR absorption intensity. A secondary effect of weakening the C=O bond is to strengthen the bonds between the carbonyl and methyl carbon atoms, leading to a blue shift in the CCC stretching frequency. There are four HCH bending deformations near 1400 cm⁻¹ whose absorptions overlap. They show minimal changes due to binding to Al^{+} . Acetone molecules in the second solvent shell are expected to have a spectrum very similar to that of bare acetone. The intensity of the photodissociation spectra of $Al^{+}(Ace)_{2.5}$ are all similar and about one order of magnitude smaller than that of $Al^{+}(Ace)(N_{2})$. This is consistent with the binding energies in Table 1, which predict that $Al^{+}(Ace)_{2.5}$ require several photons to dissociate, whereas $Al^{+}(Ace)(N_{2})$ requires only one.

Al+(**Ace**)(**N**₂). The experimental spectrum of Al⁺(Ace)(N₂) shown in figure 2 (blue) is dominated by a peak at 1627 cm⁻¹. This is to the red of the C=O stretch in isolated gas-phase acetone (1731 cm⁻¹).¹⁸ There are also weak, overlapping peaks at 1458, 1421 and 1385 cm⁻¹, which correlate to the CH₃ degenerate-deformation (1454, 1435 and 1410 cm⁻¹ in acetone) and the CH₃ symmetric-deformation (1364 cm⁻¹ in acetone), respectively. The peak at 1295 cm⁻¹ is due to the antisymmetric

CCC stretch, which is substantially blue shifted (1210 cm⁻¹ in bare acetone).¹⁸ Finally, there is a peak at \sim 1100 cm⁻¹, which is due to the CH₃ rock (1091 cm⁻¹ in bare acetone).

The calculated Al⁺-acetone binding energy is 182.1 kJ/mol, which is consistent with previous computational studies (173.6¹⁵ and 178.7⁹ kJ/mol). The calculated geometries and vibrational frequencies of Al⁺(Ace) and all of the other species discussed in this paper are in Tables S1 (B3LYP+D3) and S2 (ω B97X-D). The molecule has C_s symmetry (C_{2v} if the methyl groups rotate freely), with r_{Al-O} = 1.935 Å, r_{C-O} = 1.254 Å and r_{C-C} = 1.484 Å. The C=O bond lengthens from bare acetone (1.211 Å, calculated at this level of theory), while the C-C bonds shorten from 1.517 Å in

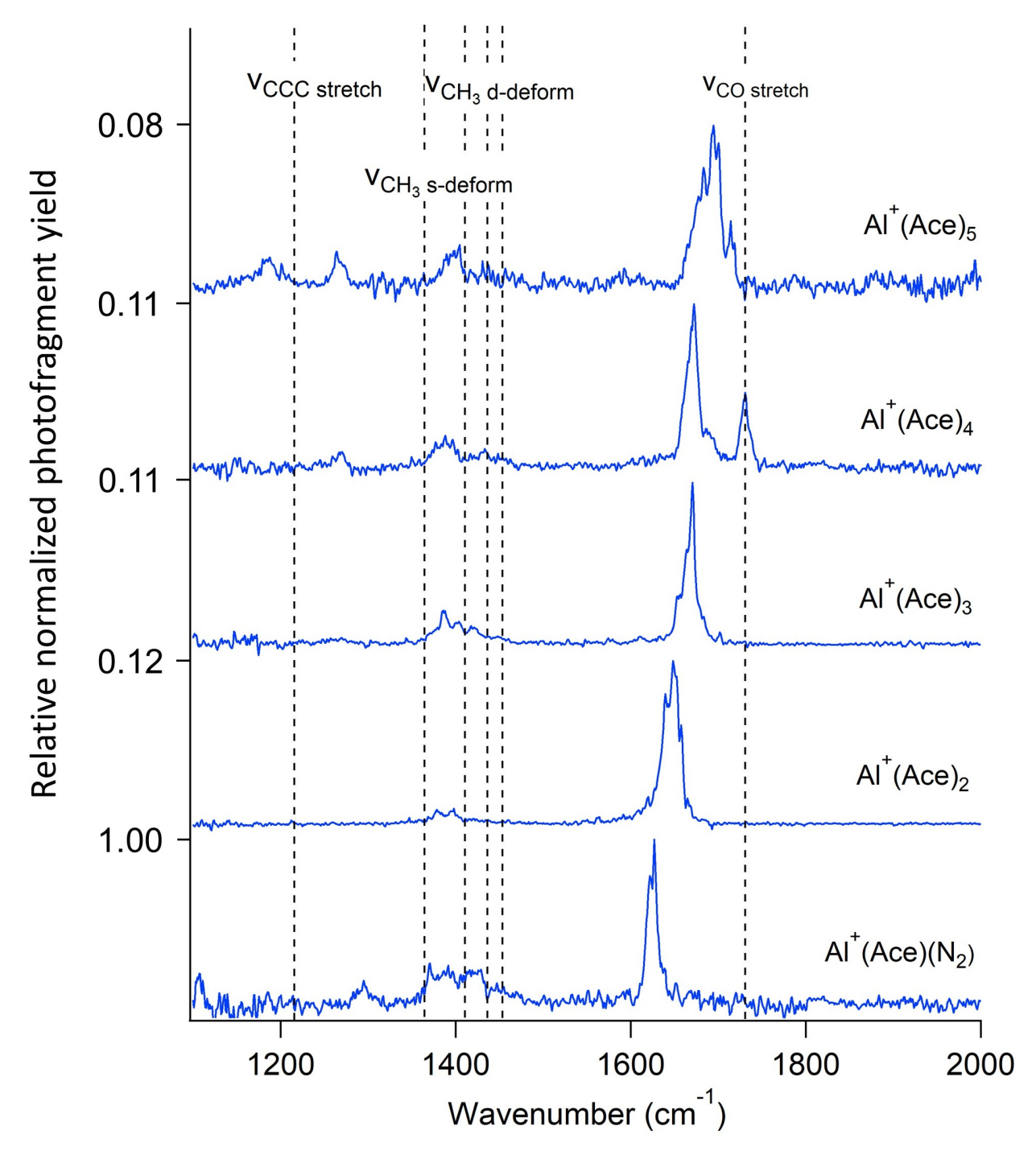


Figure 1. Vibrational spectra of $Al^+(Ace)(N_2)$ and $Al^+(Ace)_n$, where n = 2-5 from 1100 to 2000 cm⁻¹. The labels indicate stoichiometry, not the structure. The CO stretch, CCC stretch, and CH₃ deformations in bare acetone are represented by dotted vertical lines. The y-axis is the relative normalized photofragment yield compared to $Al^+(Ace)(N_2)$.

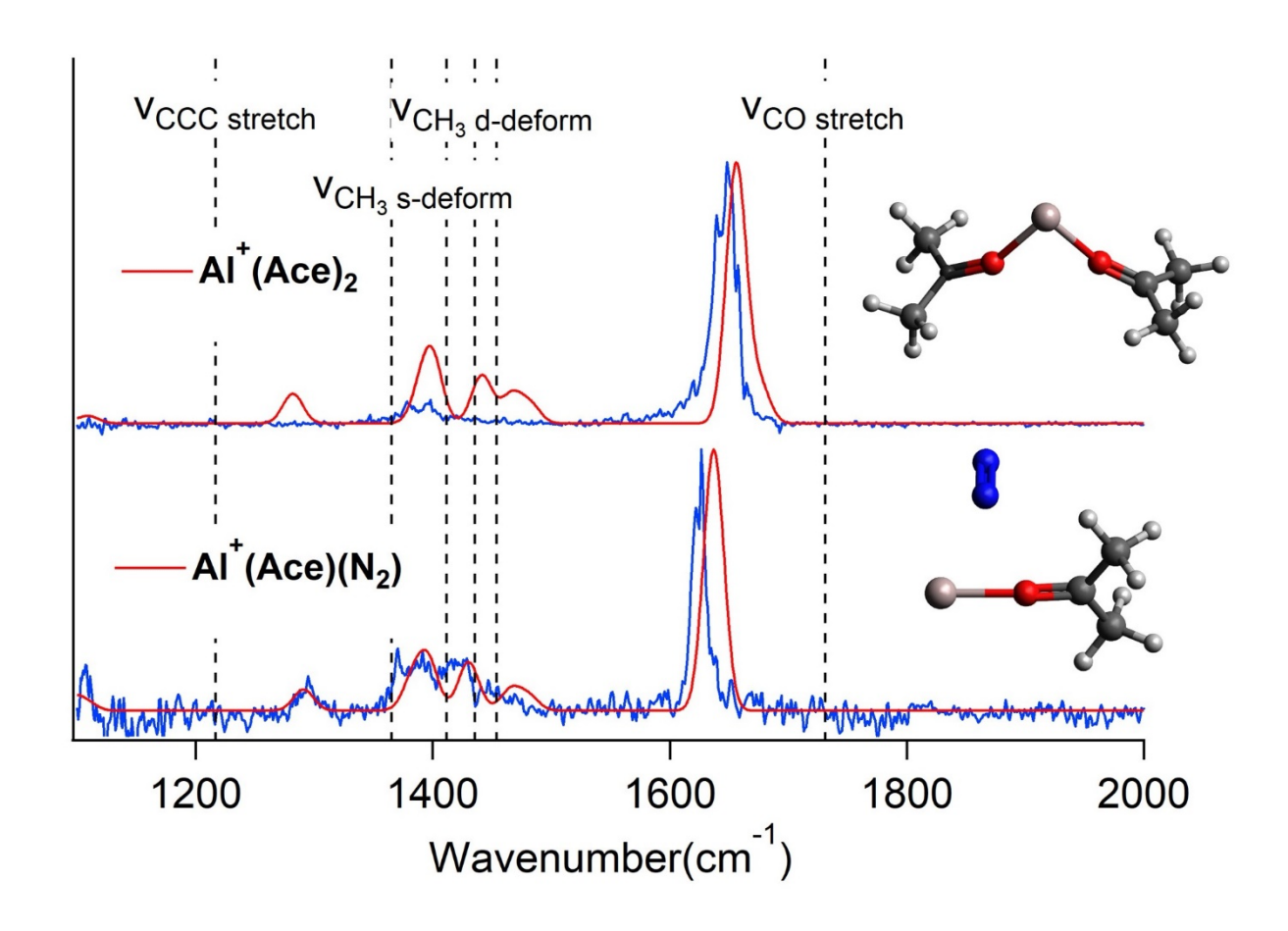


Figure 2. Experimental photodissociation spectra (blue) and simulated, B3LYP+D3/6-311+G(d,p), spectra (red) of the lowest-lying isomers of Al⁺(Ace)(N₂) and Al⁺(Ace)₂.

acetone. This is consistent with the observed shifts in the vibrational frequencies. Due to the high binding energy, the spectrum of the nitrogen-tagged molecule was measured. The calculated binding energy (10.8 kJ/mol=901 cm⁻¹) is less than the energy of one photon, so it dissociates readily. The N_2 tag binds perpendicular to the Al-O bond. The tag only slightly perturbs the calculated structure and vibrational frequencies, with $r_{C-O} = 1.251$ Å and $r_{C-C} = 1.485$ Å and ≤ 10 cm⁻¹ shifts. The simulated spectrum of Al⁺(Ace)(N_2) (Fig. 2) is an excellent match to the experimental spectrum. Velasquez *et al.*⁹ observed the C=O stretch in Al⁺(Ace)(Ar) at 1622 cm⁻¹, which is consistent with slightly less perturbation from Ar than N_2 .

Al+(**Ace**)₂. The spectrum of Al⁺(Ace)₂ (figure 2) is dominated by an intense C=O stretch peak; the CH₃ bending peaks are weak and the CCC stretch is not observed. Al⁺(Ace)₂ has a measured¹⁵ dissociation energy of 9898 cm⁻¹, and we calculate the dissociation energy to be 8978 cm⁻¹, so the spectrum is due to IRMPD. The C=O stretch (1648 cm⁻¹) is less red-shifted than for Al⁺(Ace)(N₂).

The calculations predict that the acetones bind to the same side of the Al $^+$, with an O-Al-O angle of 84.4° and $r_{Al-O} = 1.986$ Å, in agreement with previous results. This is longer than in Al $^+$ (Ace), and as a result, the acetone is less distorted, with $r_{CO} = 1.243$ Å and $r_{CC} = 1.492$ Å. Binding on the same side has been observed in complexes of Al $^+$ with ligands such as CO $_2$, C $_2$ H $_4$ and CH $_4$ $_{13.19.20}$ and is due to the ligands polarizing the 3s orbitals on Al $^+$ towards the opposite side of the metal, which allows the ligands to bind more closely to the positively charged metal, enhancing electrostatic attraction. The observed photodissociation spectrum is a good match to the calculated absorption spectrum, except that the intensities of the peaks at lower energies are lower than expected. This may be due to photodissociation being less efficient at lower energy due to lower absorption, lower laser fluence, and more photons being required to photodissociate the molecule. To investigate this, we tried to measure the spectrum of the N $_2$ or Ar-tagged molecules, but for Al $^+$ with more than one acetone, we were unable to produce sufficient parent ion signal. The Al $^+$ (Pin) isomer is calculated to be much higher in energy, and its spectrum does not match experiment (Fig. S2).

Al*(**Ace**)₃. The experimental spectrum of [AlC₉H₁₈O₃]* (nominally Al*(Ace)₃) consists of a strong peak in the C=O stretching region at 1671 cm⁻¹ and weak peaks in the CH₃ bending region (Figure 3). It is very similar to the spectrum of Al*(Ace)₂, albeit with a slightly smaller red shift in the C=O stretch. The calculations predict a trigonal pyramidal structure for Al*(Ace)₃ in which the ligands all bind to the same side of the Al*. The calculated bond lengths are $r_{Al-O} = 2.020 \text{ Å}$, $r_{C-O} = 1.243 \text{ Å}$

and $r_{C-C} = 1.491$ and 1.496 Å. These values are very similar to those in Al⁺(Ace)₂. The simulated spectrum provides a good match to experiment. However, the calculations predict that the lowest energy isomer is Al⁺(Pin)(Ace), which lies 52.5 kJ/mol below Al⁺(Ace)₃. In two of the acetone ligands, the C=O double bond becomes a single bond; a covalent Al-O bond is formed, and the central carbon atoms on each acetone form a single bond. The formal charge on the Al becomes 3+. An analogous reaction was also observed in the free-electron laser study of Nb⁺(acetonitrile)_n, where, for n=5, intramolecular reductive C–C coupling occurs, along with change of metal formal charge from 1+ to 3+.14 The calculated Mullikan charge on the Al is +0.85, which is much smaller than the formal charge, but is still significantly higher than in Al⁺(Ace)₃ (+0.41), so the acetone is more strongly bound and the C=O stretch in the acetone is substantially more red shifted. The vibrational spectrum of pinacol (2,3-dimethyl-2,3-butanediol)²² is very similar to that of acetone, except for a distinctive peak near 1170 cm⁻¹ which corresponds to the C-O stretch. In our calculated spectrum of Al⁺(Pin)(Ace) this appears at 1145/1147 cm⁻¹. This peak is not observed in the experiment. So, although Al+(Pin)(Ace) is the lowest energy isomer, it does not appear to contribute to the experimental spectrum. This is due to two reasons. First and foremost, there is a 100.7 kJ/mol barrier to forming Al⁺(Pin)(Ace) from Al⁺(Ace)₂ + acetone (Figure S3). Second, loss of acetone from Al⁺(Pin)(Ace) is highly endothermic, by 10885 cm⁻¹ to form Al⁺(Ace)₂ + acetone and 28921 cm⁻¹ to Al⁺(Pin) + acetone, so photodissociation would be very inefficient.

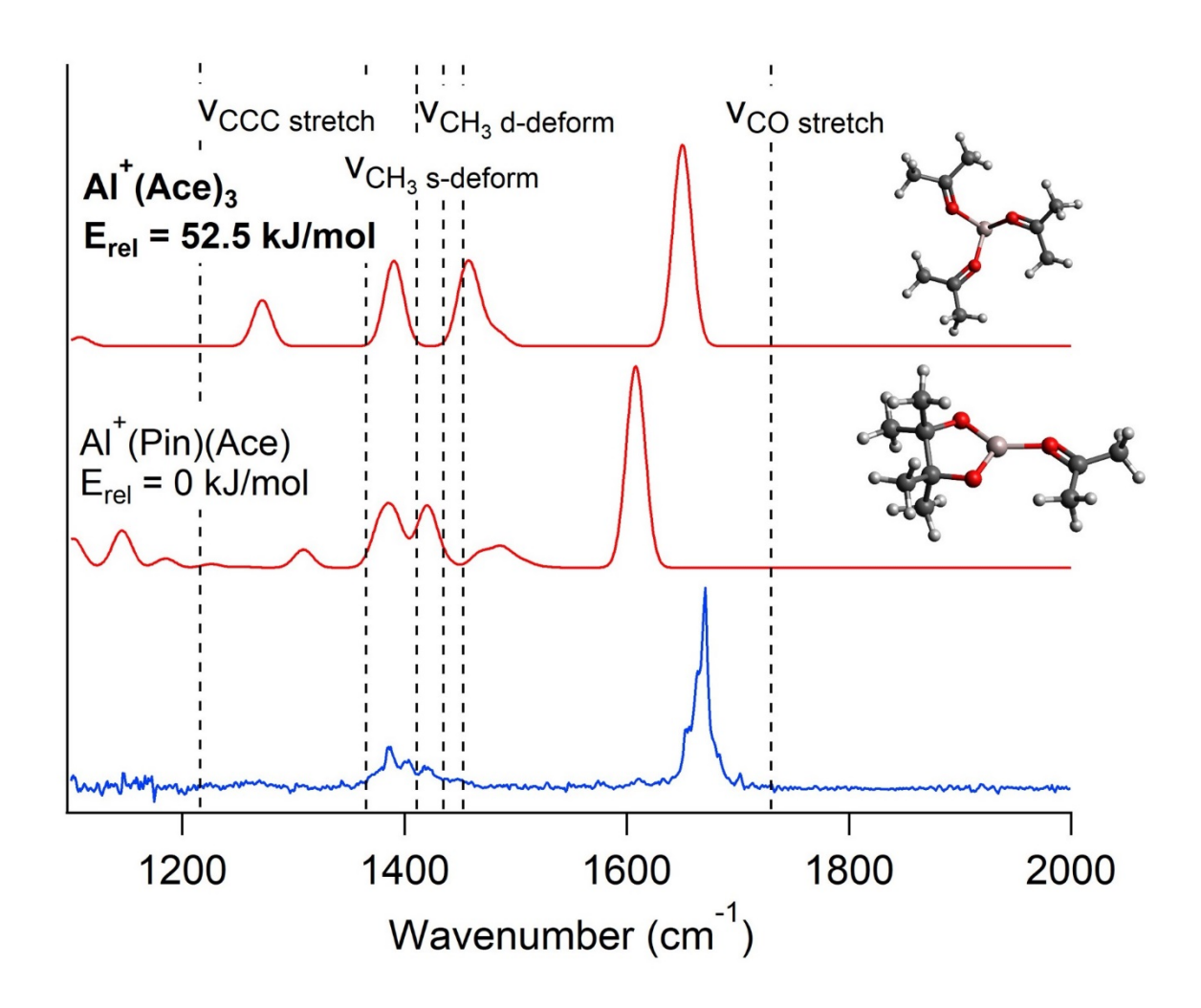


Figure 3. Experimental photodissociation spectrum (blue), simulated spectra of two low-lying isomers (red), and optimized geometries of $[AlC_9H_{18}O_3]^+$ at the B3LYP+D3/6-311+G(d,p) level of theory.

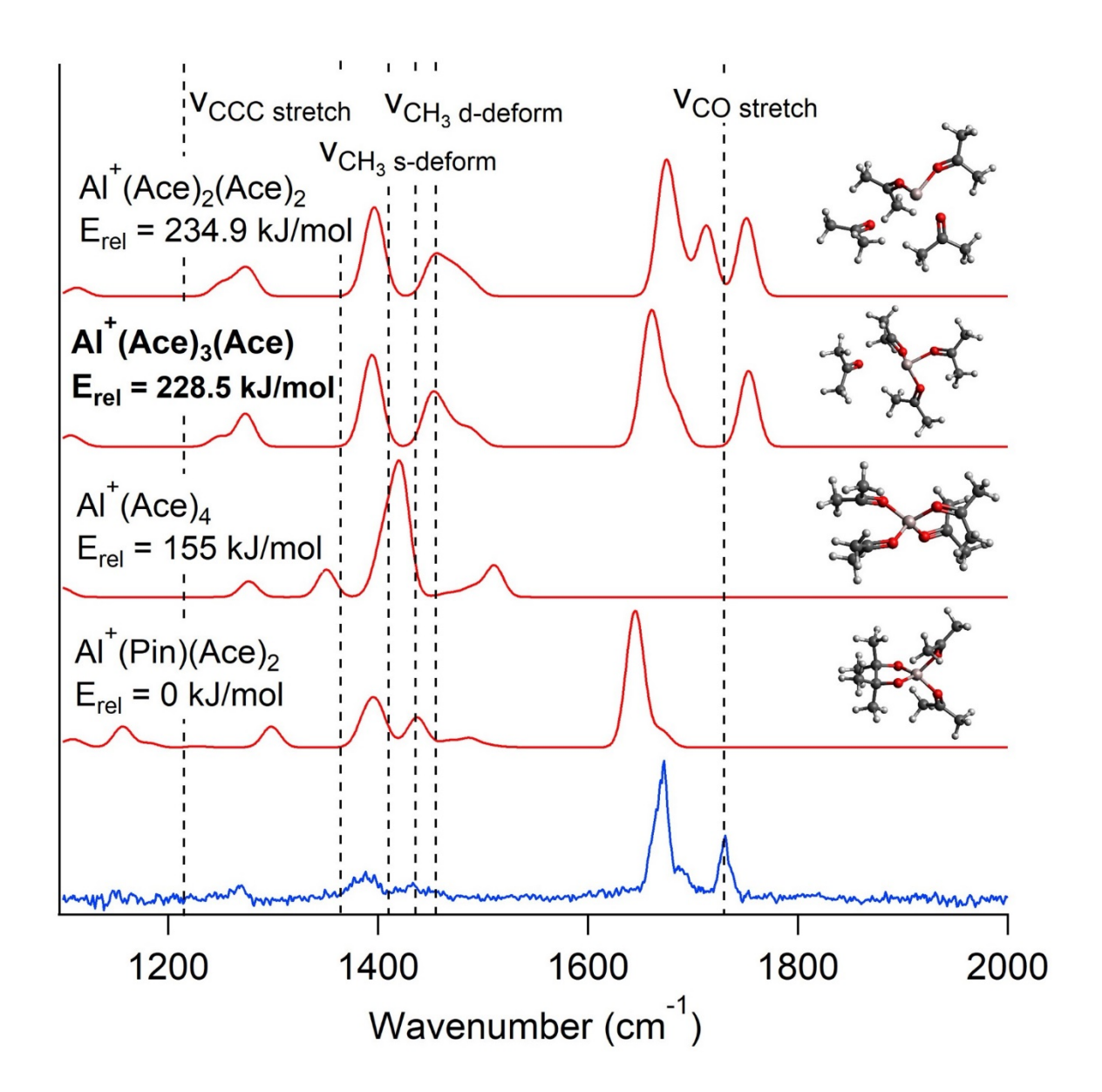


Figure 4. Experimental photodissociation spectrum (blue), simulated spectra of four low-lying isomers, and optimized geometries of $[AlC_{12}H_{24}O_4]^+$ at the B3LYP+D3/6-311+G(d,p) level of theory.

Al*(Ace)₃(Ace) and isomers. The experimental spectrum (Figure 4) contains two strong peaks in the C=O stretching region at 1672 and 1731 cm⁻¹. The peak at 1731 cm⁻¹ shows no red shift from isolated acetone, which indicates that at least one acetone molecule is not directly coordinated to the Al*. The peak at 1672 cm⁻¹ is only 1 cm⁻¹ away from the peak in Al*(Ace)₃ and, again, is due to acetone(s) coordinated to Al*. We also consider the possibility that the peak at 1731 cm⁻¹ is due to an overtone or combination band which gains intensity due to mixing with and borrowing intensity from the nearby C=O stretch fundamental. However, this is unlikely, as no analogous peak is observed for Al*(Ace)₃ or Al*(Pin)(Ace)₃, despite them having similar C=O stretching frequencies to the n=4 cluster. As with the smaller clusters, HCH bending peaks are observed at 1452, 1433 and 1388 cm⁻¹ and there is a peak at 1270 cm⁻¹ due to the CCC stretch.

The calculations show that the lowest energy isomer is a pinacolate with two acetones bound to the metal. However, the simulated spectrum does not contain a peak near 1731 cm⁻¹, so it cannot be the only isomer observed. The next lowest-energy isomer, Al⁺(Ace)₄, is a symmetrical structure in which there is a partial Al-O bond, the C=O bond is weakened, and there is some radical character on the central carbon. In some ways, it is a precursor to a pinacolate. As a result, the C=O stretch is very red shifted, and the predicted spectrum bears no resemblance to the experiment. The next isomer, Al⁺(Ace)₃(Ace) has three ligands bound to the metal, with the fourth in the second solvent shell. As a result, the spectrum is similar to that of Al⁺(Ace)₃, with an additional peak in the free acetone C=O region. It is an excellent match to the observed spectrum. A final isomer, Al⁺(Ace)₂(Ace)₂ is similar, but with two first-shell ligands and two in the second shell. The predicted spectrum is also similar, but three well-separated C=O peaks are predicted, and only two (plus a shoulder near 1687 cm⁻¹) are observed. It is challenging to determine whether Al⁺(Pin)(Ace)₂ is also formed, as most of its calculated spectrum overlaps that of Al⁺(Ace)₃(Ace).

The most distinctive peak is calculated to lie at 1158 cm⁻¹ and is due to the C-O stretch. This region of the spectrum is magnified in Figure S4, and there is no clear peak observed, so we have no evidence that Al⁺(Pin)(Ace)₂ is formed.

It is surprising that the observed spectrum is due to an isomer that is calculated to be at such a high energy (228.5 kJ/mol). Reaction of Al⁺(Ace)₃ with acetone will initially form Al⁺(Ace)₃(Ace). As shown in Figure S5, the calculations then predict that there is a submerged barrier 30 kJ/mol below Al⁺(Ace)₃ + acetone in order to form Al⁺(Ace)₄. There is a second barrier, 25 kJ/mol below reactants, in order to then produce Al⁺(Pin)(Ace)₂. The experiment clearly shows that some of reactants are trapped in the Al⁺(Ace)₃(Ace) entrance channel. It is possible that we are also forming Al⁺(Pin)(Ace)₂, but the acetone binding energy is so high (18552 cm⁻¹) that it doesn't photodissociate.

Groenewold et al.¹⁰ studied structure and bonding in $UO_2^{2+}(Ace)_n$ (n=2-4), measuring their vibrational spectrum. The C=O stretch is observed at 1500/1527 cm⁻¹, 1583 cm⁻¹, and 1630 cm⁻¹ for n=2 to 4. All of the acetones are bound to the metal. These red shifts are substantially larger than those of the Al⁺ complexes, likely due to the higher charge on the cation. In both cases, the red shifts decrease as acetones are added. In $UO_2^{2+}(Ace)_4$, the CCC stretch is at 1249 cm⁻¹. This is blue shifted from bare acetone, but the blue shift is smaller than we observe for Al⁺(Ace)₃(Ace), 1270 cm⁻¹. The $UO_2^{2+}(Ace)_n$ do not have a peak near 1170 cm⁻¹, indicating that pinacolates are not formed.

Al⁺(**Pin**)(**Ace**)₃ and isomers. As shown in figure 5, the experimental spectrum of [AlC₁₅H₃₀O₅]⁺ shows a broad peak at 1690 cm⁻¹, characteristic of a C=O stretch of acetone bound to Al⁺. This peak is about twice as wide as in the smaller clusters, suggesting that the acetones are not

equivalent or that multiple isomers contribute to the spectrum. It is noteworthy that there is no peak in the free C=O region (1731 cm⁻¹). There are the typical peaks in the CH₃ deformation region (the largest at 1404 cm⁻¹), and the blue-shifted CCC stretch in acetone bound to Al⁺ is observed at 1280 cm⁻¹. There is a peak at 1185 cm⁻¹ that is not observed in the smaller clusters.

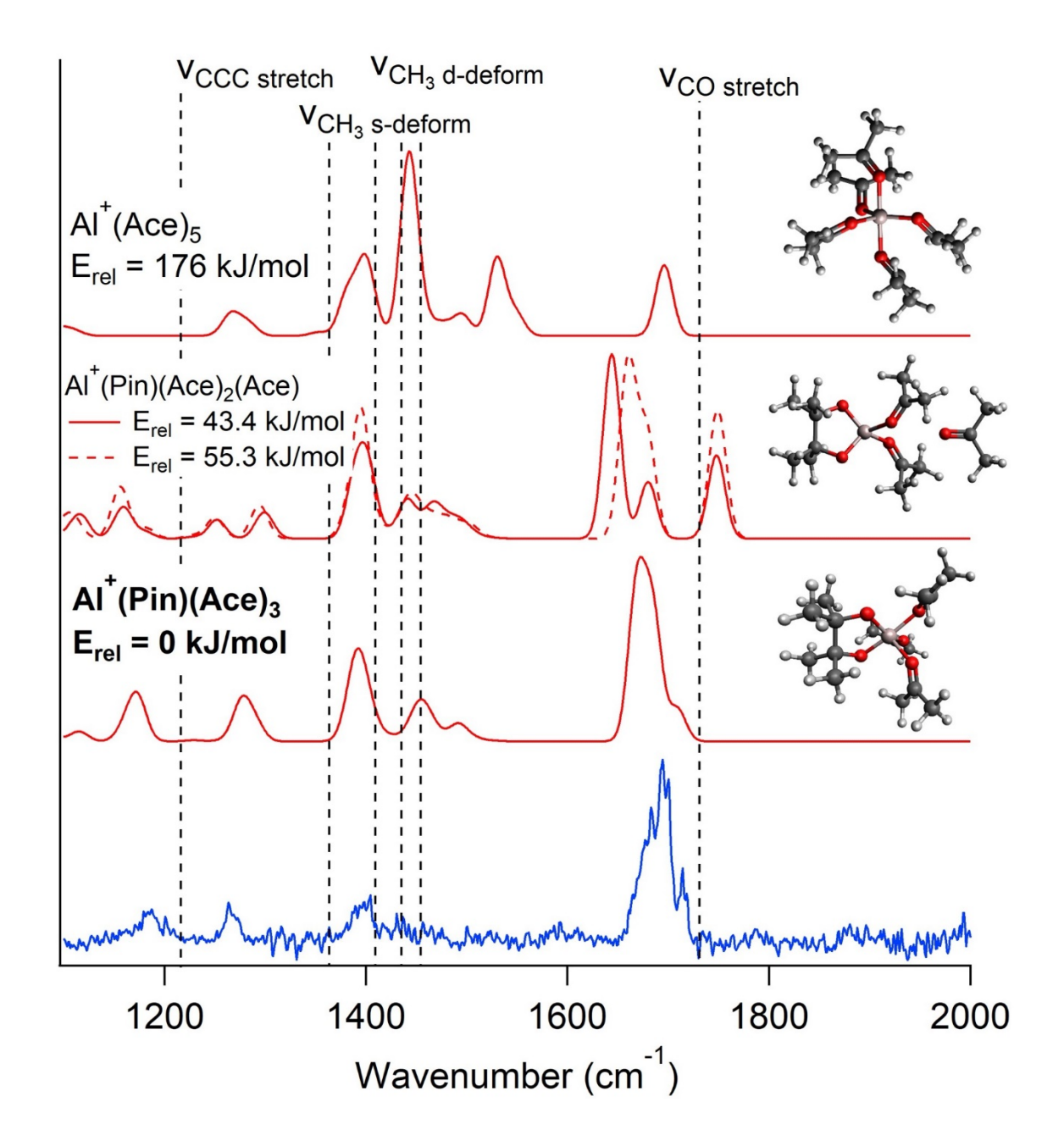


Figure 5. Experimental photodissociation spectrum (blue), simulated spectra of four low-lying isomers, and optimized geometries of $[AlC_{15}H_{30}O_5]^+$ at the B3LYP+D3/6-311+G(d,p) level of theory. The higher-energy $Al^+(Pin)(Ace)_2(Ace)$ isomer is not shown.

The lowest-energy isomer is a pinacolate, $Al^+(Pin)(Ace)_3$. The pinacolate has $r_{C-C} = 1.589$ Å, $r_{C-O} = 1.44$ Å and $r_{Al-O} = 1.76$ -1.78 Å. The formal charge on the Al is 3+ (the Mullikan charge is 1.315). There are three, inequivalent, acetone ligands bound to the Al. They have $r_{Al-O} = 1.92$ -1.95 Å and $r_{C-O} = 1.242$ -1.244 Å. The simulated spectrum (Fig. 5) is an excellent match to experiment. Because the acetones are not equivalent, the C=O stretches range from 1675 to 1706 cm⁻¹, leading to a broad peak. The C-O stretch in the pinacolate is calculated to be at 1173 cm⁻¹, and is an excellent match to the peak observed at 1185 cm⁻¹. This peak is diagnostic of the presence of a pinacolate. The $Al^+(Pin)(Ace)_2$ – Ace binding energy is calculated to be 8532 cm⁻¹, which is substantially less than for $Al^+(Pin)(Ace)$ – Ace.

The next lowest-lying isomers, Al⁺(Pin)(Ace)₂(Ace) are similar, but have a second shell acetone. They are predicted to have a peak in the free C=O region, which is not observed. At higher energy, there is a distorted trigonal bipyramidal structure, Al⁺(Ace)₅. The predicted spectrum is also not a good match to experiment.

The vibrational spectrum confirms that reaction of Al^+ with five acetone molecules leads to C-C coupling and the formation of a pinacolate. Although the pinacolate is also thermodynamically favored for reaction with three and four acetones, we don't observe it, likely due to high barriers to its formation, or to high acetone binding energy inhibiting photodissociation. Additional acetone molecules facilitate the reaction by crowding those bound to the meal so they are closer together. In addition, the higher charge on the metal following the electron transfer leads to stronger bonds with the remaining acetones. A similar intracluster reaction coupling electron transfer and C-C bond formation in carbonyls has also been observed in $V^+(CO_2)_n$, with formation of oxalate,²³ but not in $Al^+(CO_2)_n$. In both cases, additional solvent molecules (acetone or CO_2) facilitate the

reaction, but for $V^+(CO_2)_n$, a second solvent shell is required. This class of reactions in $M^+(ligand)_n$ clusters is likely to occur for metals that can adopt a 3+ oxidation state.

In conclusion, vibrational spectra of $Al^+(Ace)(N_2)$ and ions with the stoichiometry of $Al^+(Ace)_n$ (n=2-5) were measured from 1100 to 2000 cm⁻¹ by monitoring loss of N_2 or acetone. Compared to isolated acetone, the spectra show a red shift in the C=O stretch that decreases as the size of the cluster increases and a blue shift in the CCC stretch that decreases with increasing cluster size. Calculations predict that for n=3-5 the most stable isomer is a pinacolate structure: $[Al(Pin)(Ace)_n]^+$ in which the Al is formally in the 3+ oxidation state. Experimentally, the isomer observed is $Al^+(Ace)_3$ for n=3 and $Al^+(Ace)_3$ (Ace) for n=4. For n=5, there is clear evidence for pinacolate formation, $Al^+(Pin)(Ace)_3$.

Experimental and Computational Methods

The desired clusters are produced and their spectra are measured on a home-built dual time-of-flight reflectron mass spectrometer.²⁴ The stoichiometric Al*(Ace)_n, where n = 1-5, are produced in a laser vaporization source. Nd:YAG (532 nm) laser ablation of an aluminum rod forms Al*. A pulsed valve introduces a mixture of 0.25 to 0.6% acetone/20% Ar/80% He at 20 psi backing pressure to produce the ion of interest. For N₂-tagged ions, a 0.07% acetone/5% Ar/10% N₂/85% He mix is used. The ions then are cooled to a rotational temperature of ~15K by expansion into a vacuum chamber and are injected into a reflectron time-of-flight mass spectrometer. The mass-selected ions are irradiated with a pulse of infrared light, which makes ~10 passes through the ion cloud.²⁵ IR light tunable from 1100 to 2000 cm⁻¹ (the fingerprint region) is produced by a Nd:YAG-pumped (1064 nm) OPO/OPA IR laser system (LaserVision) coupled to a AgGaSe₂ crystal. The laser produces 0.25 mJ/pulse near 2000 cm⁻¹, with a line width of ~2 cm⁻¹. the wavelength is

calibrated using the methane absorption spectrum.²⁶ The vibrational spectrum of the clusters is measured by monitoring fragment ion signal as a function of IR wavenumber to provide information about structure and bonding.

To determine isomeric structures, optimized geometries and vibrational spectra are calculated using density functional theory (DFT). Calculations using the Gaussian09 program²⁷ were carried out at the B3LYP+D3/6-311+G(d,p) and ω B97X-D/6-311+G(d,p) levels of theory. Vibrational frequencies are not scaled and all reported energies include zero-point energies. Simulated spectra are calculated by convoluting the calculated stick spectrum with a Gaussian with 20 cm⁻¹ fwhm.

ASSOCIATED CONTENT

Supporting Information

The Supporting Information is available free of charge at (url inserted by journal).

Full ref. 25; mass spectrum (Fig. S1); Experimental and calculated vibrational spectra of low-lying isomers of Al⁺(Ace)₂ (Fig. S2); Potential energy surface for Al⁺(Ace)₂ + acetone and Al⁺(Ace)₃ + acetone calculated at the B3LYP+D3/6-311+G(d,p) level of theory (Figs. S3 and S5); Experimental vibrational spectra highlighting the region below the carbonyl stretch and simulated spectra of low-lying pinacolate isomers (Fig. S4); Energies, geometries, vibrational frequencies and intensities of Al⁺(Ace)(N₂) and the isomers of stoichiometric Al⁺(Ace)_n, at the B3LYP+D3/6-311+G(d,p) level of theory (Table S1) and ω B97X-D/6-311+G(d,p) (Table S2) (PDF).

AUTHOR INFORMATION

Corresponding Author

Ricardo B. Metz - Department of Chemistry, University of Massachusetts Amherst, Amherst, Massachusetts 01003, United States; https://orcid.org/0000-0003-1933-058X; rbmetz@chem.umass.edu

Author

Apakorn Phasuk - Department of Chemistry, University of Massachusetts Amherst, Amherst, Massachusetts 01003, United States; https://orcid.org/0000-0002-6758-857X; aphasuk@chem.umass.edu

Notes

The authors declare no competing financial interests.

ACKNOWLEDGMENTS

Financial support from the National Science Foundation under award no. CHE-2154391 is gratefully acknowledged. AP is supported by a Development and Promotion of Science and Technology Talents Project, Thai government scholarship. The authors are grateful for computational resources provided by the Massachusetts Green High-Performance Computing Center (MGHPCC).

REFERENCES

- (1) Terra, B. S.; MacEdo, F. Progress in Intermolecular Pinacol Cross Coupling Methodologies. *Arkivoc* **2012**, *2012*, 134–151.
- (2) Li, C.-J. Organic Reactions in Aqueous Media with a Focus on Carbon-Carbon Bond Formations: A Decade Update. *Chem. Rev.* **2005**, *105*, 3095–3165.
- (3) Rieke, R. D.; Kim, S. New Reagent for Reductive Coupling of Carbonyl and Imine

- Compounds: Highly Reactive Manganese-Mediated Pinacol Coupling of Aryl Aldehydes, Aryl Ketones, and Aldimines. *J. Org. Chem.* **1998**, *63*, 5235–5239.
- (4) Hirao, T. Catalytic Reductive Coupling of Carbonyl Compounds The Pinacol Coupling Reaction and Beyond. *Top. Curr. Chem.* **2007**, 279, 53–75.
- (5) Li, L. H.; Chan, T. H. Effect of Fluoride Salts on Metal-Mediated Reactions.

 Aluminum/Fluoride Salt-Mediated Reduction and Pinacol Coupling of Carbonyl

 Compounds in Aqueous Media. *Org. Lett.* **2000**, *2*, 1129–1131.
- (6) Asmis, K. R. Structure Characterization of Metal Oxide Clusters by Vibrational Spectroscopy: Possibilities and Prospects. *Phys. Chem. Chem. Phys.* **2012**, *14*, 9270–9281.
- (7) Song, X.; Fagiani, M. R.; Gewinner, S.; Schöllkopf, W.; Asmis, K. R.; Bischoff, F. A.; Berger, F.; Sauer, J. Gas Phase Structures and Charge Localization in Small Aluminum Oxide Anions: Infrared Photodissociation Spectroscopy and Electronic Structure Calculations. *J. Chem. Phys.* **2016**, *144*.
- (8) Roithova, J. Characterization of Reaction Intermediates by Ion Spectroscopy. *Chem. Soc. Rev.* **2012**, *41*, 547–559.
- (9) Velasquez, J.; Pillai, E. D.; Carnegie, P. D.; Duncan, M. A. IR Spectroscopy of M⁺(Acetone) Complexes (M = Mg, Al, Ca): Cation-Carbonyl Binding Interactions. *J. Phys. Chem. A* **2006**, *110*, 2325–2330.
- (10) Groenewold, G. S.; Gianotto, A. K.; Cossel, K. C.; Van Stipdonk, M. J.; Moore, D. T.; Polfer, N.; Oomens, J.; De Jong, W. A.; Visscher, L. Vibrational Spectroscopy of Mass-

- Selected $[UO_2(Ligand)_n]^{2+}$ Complexes in the Gas Phase: Comparison with Theory. *J. Am. Chem. Soc.* **2006**, *128*, 4802–4813.
- (11) Groenewold, G. S.; Gianotto, A. K.; Cossel, K. C.; Van Stipdonk, M. J.; Oomens, J.; Polfer, N.; Moore, D. T.; De Jong, W. A.; McIlwain, M. E. Mid-Infrared Vibrational Spectra of Discrete Acetone-Ligated Cerium Hydroxide Cations. *Phys. Chem. Chem. Phys.* 2007, 9, 596–606.
- (12) Vaden, T. D.; Lisy, J. M. Investigation of Competing Interactions in Alkali Metal Ion-Acetone-Water Clusters. *Chem. Phys. Lett.* **2005**, *408*, 54–58.
- (13) Walker, N. R.; Walters, R. S.; Duncan, M. A. Infrared Photodissociation Spectroscopy of Al⁺(CO₂)_n and Al⁺(CO₂)_nAr Complexes. *J. Chem. Phys.* **2004**, *120*, 10037–10045.
- (14) Reinhard, B. M.; Lagutschenkov, A.; Lemaire, J.; Maitre, P.; Boissel, P.; Niedner-Schatteburg, G. Reductive Nitrile Coupling in Niobium-Acetonitrile Complexes Probed by Free Electron Laser IR Multiphoton Dissociation Spectroscopy. *J. Phys. Chem. A* **2004**, *108*, 3350–3355.
- (15) Bauschlicher Jr., C. W.; Bouchard, F.; Hepburn, J. W.; McMahon, T. B.; Surjasasmita, I.; Roth, L. M.; Gord, J. R.; Freiser, B. S. On the Structure of Al(Acetone)₂⁺. *Int. J. Mass Spectrom. Ion Process.* **1991**, *109*, 15–30.
- (16) Gal, J. F.; Yáñez, M.; Mó, O. Aluminum Monocation Basicity and Affinity Scales. Eur. J. Mass Spectrom. 2015, 21, 517–532.
- (17) Bouchard, F.; Brenner, V.; Carra, C.; Hepburn, J. W.; Koyanagi, G. K.; McMahon, T. B.;

- Ohanessian, G.; Peschke, M. Energetics and Structure of Complexes of Al⁺ with Small Organic Molecules in the Gas Phase. *J. Phys. Chem. A* **1997**, *101*, 5885–5894.
- (18) Shimanouchi, T. Tables of Molecular Vibrational Frequences Consolidated, Vol. 1. *Natl. Bur. Stand.* **1972**, 1–16.
- (19) Yuan, J.; Zhao, Y.; Hou, G.; Gao, Z.; Zheng, W. Structures of Al⁺(C₂H₄)_n Clusters: Mass-Selected Photodissociation and Ab Initio Calculations. *Int. J. Mass Spectrom.* **2012**, *309*, 49–55.
- (20) Poad, B. L. J.; Thompson, C. D.; Bieske, E. J. Infrared Spectra of Mass-Selected Al⁺-(CH₄)_n $n = 1-6 \text{ Clusters. } Chem. Phys. \ \textbf{2008}, 346, 176-181.$
- (21) Sodupe, M.; Bauschlicher Jr., C. W. Al⁺—Ligand Binding Energies. *Chem. Phys. Lett.* **1991**, *181*, 321–326.
- (22) Wallace, W. E. "Infrared Spectra"; in NIST Chemistry WebBook, NIST Standard Reference Database Number 69, Eds. P.J. Linstrom and W.G. Mallard, National Institute of Standards and Technology: Gaithersburg MD, 20899.
- (23) Ricks, A. M.; Brathwaite, A. D.; Duncan, M. A. IR Spectroscopy of Gas Phase V(CO₂)_n⁺ Clusters: Solvation-Induced Electron Transfer and Activation of CO₂. *J. Phys. Chem. A* **2013**, *117*, 11490–11498.
- (24) Husband, J.; Aguirre, F.; Ferguson, P.; Metz, R. B. Vibrationally Resolved Photofragment Spectroscopy of FeO+. *J. Chem. Phys.* **1999**, *111*, 1433–1437.
- (25) Kaur, D.; de Souza, A. M.; Wanna, J.; Hammad, S. A.; Mercorelli, L.; Perry, D. S. Multipass

- Cell for Molecular Beam Absorption Spectroscopy. Appl. Opt. 1990, 29, 119–124.
- (26) Gordon, I. E.; Rothman, L. S.; Hill, C.; Kochanov, R. V.; Tan, Y.; Bernath, P. F.; Birk, M.;
 Boudon, V.; Campargue, A.; Chance, K. V.; Drouin, B. J.; Flaud, J. M.; Gamache, R. R.;
 Hodges, J. T.; Jacquemart, D.; Perevalov, V. I.; Perrin, A.; Shine, K. P.; Smith, M. A. H.;
 Tennyson, J.; Toon, G. C.; Tran, H.; Tyuterev, V. G.; Barbe, A.; Császár, A. G.; Devi, V.
 M.; Furtenbacher, T.; Harrison, J. J.; Hartmann, J. M.; Jolly, A.; Johnson, T. J.; Karman, T.;
 Kleiner, I.; Kyuberis, A. A.; Loos, J.; Lyulin, O. M.; Massie, S. T.; Mikhailenko, S. N.;
 Moazzen-Ahmadi, N.; Müller, H. S. P.; Naumenko, O. V.; Nikitin, A. V.; Polyansky, O. L.;
 Rey, M.; Rotger, M.; Sharpe, S. W.; Sung, K.; Starikova, E.; Tashkun, S. A.; Auwera, J.
 Vander; Wagner, G.; Wilzewski, J.; Wcisło, P.; Yu, S.; Zak, E. J. The HITRAN2016
 Molecular Spectroscopic Database. J. Quant. Spectrosc. Radiat. Transf. 2017, 203, 3–69.
- (27) Frisch, M. J.; Trucks, G. W.; Schlegel, H. B.; Scuseria, G. E.; Robb, M. A.; Cheeseman, J. R.; Scalmani, G.; Barone, V.; Petersson, G. A.; Nakatsuji, H.; Li, X.; Caricato, M.; Marenich, A.; Bloino, J.; Janesko, B. G.; Gomperts, R.; Mennucci, B.; . et. al. Gaussian09. *Revision D.01*. Gaussian Inc: Wallingford CT **2013**.